Blood Flow through a Composite Stenosis
in an Artery with Permeable Wall

Shailesh Mishra[1], S.U. Siddiqui[2] and Amit Medhavi[3]

[1]Department of Mathematics
Krishna Girls Engineering College
Kanpur-209217, India
shailesh27sep@rediffmail.com

[2]Department of Mathematics
H.B.T.I.
Kanpur-208002, India
susiddmath@yahoo.com

[3]Department of Mechanical Engineering
Kamla Nehru Institute of Technology
Sultanpur-228118, India
amitmedhavi@yahoo.co.in

Abstract

The present work concerns the fluid mechanical study on the effects of the permeability of the wall through an artery with a composite stenosis. The expressions for the blood flow characteristics, the flow resistance, the wall shear stress, shearing stress at the stenosis throat have been derived. Results for the effect of permeability on these flow characteristics are shown graphically and discussed briefly.

1. Introduction

The frequently occurring cardiovascular disease, stenosis or arteriosclerosis is the abnormal and unnatural growth in the arterial wall thickness that develops at various locations of the cardiovascular system under diseased conditions and occasionally results into serious consequences (cerebral strokes, myocardial infarction, angina pectoris, cardiac arrests, etc.). It is believed that deposits of cholesterol, fatty substances, cellular waste products, calcium, and fibrin may be responsible for the development of the disease. Regardless of the cause, it is known that once an obstruction has developed, it results into significant changes in pressure distribution, wall shear stress and impedance (flow resistance).

In the constricted region, the flow accelerates and consequently the velocity gradient near the wall region is steeper due to the increased core velocity resulting relatively large shear stress on the wall even for a mild stenosis. The knowledge that hemodynamic factors play an important role in the genesis of the disease, since the first investigation of Mann et al. (1938), a large number of researchers including [Young (1968), (1979); Young and Tsai (1973); Caro et al. (1978); Shukla et al. (1980); Ahmed and Giddens (1983); Sarkar and Jayaraman (1998); Pralhad and Schultz (2004); Jung et al. (2004); Liu et al. (2004); Srivastava and coworkers (1996, 2009, 2010a,b,c); Mishra et al. (2006); Misra and Verma (2007); Ponalagusamy (2007); Layek et al. (2005), (2009); Joshi et al. (2009); Mekheimer and El-Kot (2008); Tzirtzilakis (2008); Mandal and coworkers (2005), (2007a,b); Politis et al. (2007, 2008); and Singh et al. (2010)] and many others, have addressed the problem in various contexts.

It is well established fact that endothelial walls are permeable with ultra microscopic pores through which filtration occurs. Cholesterol is believed to increase the permeability of the arterial wall. Such increase in permeability results from dilated, damaged or inflamed arterial walls. It is worthwhile to study the effects of permeability of the wall of an arteriosclerotic blood vessel. Due to the permeability of the arterial wall, the no slip condition at the wall is no longer valid and one has to consider a slip condition at the artery wall. A survey of the literature indicates that the majority of the investigations, reported so far, have considered axisymmetric and non-symmetric single stenoses. However, in realistic situations stenosis may develop in series (multiple stenosis), overlapping or of composite in nature [Srivastava et al. (2010b)]. In view of the discussion given above the present research is devoted to study the flow of blood through a stenotic artery with permeable wall.

The flow in the permeable boundary is described by Darcy law which states that the rate at which a fluid flows through a permeable substance per unit area is equal to the permeability (a property of the substance through which the fluid is flowing) times the pressure drop per unit length of flow, divided by the viscosity of the fluid. Blood is assumed to be represented by a Newtonian fluid and to generalize the problem further the shape of the stenosis is considered to be composite in nature. The wall in the vicinity of the stenosis is usually solid when stenosis develops in living vasculature. Further, to neglect the entrance, end and special wall effects the artery length is considered large enough as compared to its radius.

2. Formulation of the Problem

Consider the axisymmetric flow of blood through a composite stenosis in a circular tube with permeable wall specified at the position as shown in Fig.1. The geometry of the stenosis, assumed to be manifested in the arterial segment, is described [Joshi et al. (2009): Srivastava et al. (2010b)] as

$$R(z)/R_0 = 1 - \frac{2\delta}{R_0 L_0}(z - d); \quad d \le z \le d + L_0/2, \tag{1}$$

$$= 1 - \frac{\delta}{2R_0}\left\{1 + \cos\frac{2\pi}{L_0}(z - d - L_0/2)\right\}; d + L_0/2 \le z \le d + L_0, \tag{2}$$

$$= 1, \quad \text{otherwise}, \tag{3}$$
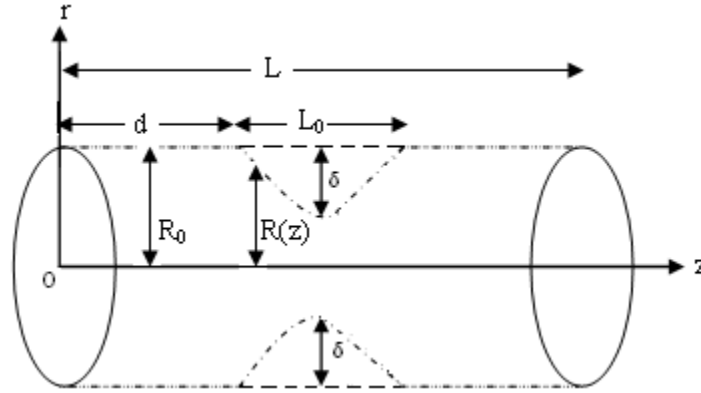
Figure1. Flow geometry of a composite stenosis in an artery with permeable wall

where $R \approx R(z)$ is the artery radius in the obstructed region, R_0 is the radius of the normal artery, L_0 is the stenosis length and d indicates its location, δ is the maximum projection (height of the throat) of the stenosis located at $z = d + L_0/2$, z being the axial coordinate.

Assuming that the flowing blood is represented by a Newtonian fluid and considering the axisymmetric, laminar, steady one-dimensional fully developed flow of blood in an artery, the equations governing the flow in the case of a mild stenosis ($\delta \ll R_0$) may therefore be written [Young (1968), Srivastava and Rastogi (2009)] as

$$\frac{dp}{dz} = \frac{1}{r}\frac{\partial}{\partial r}\left(r\mu\frac{\partial u}{\partial r}\right), \tag{4}$$

$$\frac{dp}{dr} = 0, \tag{5}$$

where u is the axial velocity, μ is the fluid viscosity, r is the radial coordinate and p is the pressure.

The boundary conditions [Beavers and Joseph (1967)] are

$$\frac{\partial u}{\partial r} = 0 \; at \; r = 0, \tag{6}$$

$$u = u_B \quad and \quad \frac{\partial u}{\partial r} = \frac{\alpha}{\sqrt{D_a}} (u_B - u_{porous}) \quad at \; r = R(z), \tag{7}$$

where $u_{porous} = -\dfrac{D_a}{\mu} \dfrac{dp}{dz}$, u_{porous} is the velocity in the permeable boundary, u_B is the slip velocity,

D_a is the Darcy number and α (called the slip parameter) is a dimensionless quantity depending on the material parameters which characterize the structure of the permeable material within the boundary region.

3. Analysis

The expression for the velocity, obtained as the solution of equations (4) and (5) subject to the boundary conditions (6) and (7), is given as

$$u = -\frac{1}{4\mu} \frac{dp}{dz} (R^2 - r^2) + u_B, \tag{8}$$

where the slip velocity, u_B is determined as

$$u_B = \frac{\sqrt{D_a}}{2\mu \, \alpha} \frac{dp}{dz} \left\{ R_0 \left(\frac{R}{R_0} \right) - 2\alpha \sqrt{D_a} \right\}. \tag{9}$$

An application of equation (9) in to (8), yields

$$u = -\frac{1}{4\mu} \frac{dp}{dz} (R^2 - r^2) + \frac{\sqrt{D_a}}{2\mu \, \alpha} \frac{dp}{dz} \left\{ R_0 \left(\frac{R}{R_0} \right) - 2\alpha \sqrt{D_a} \right\}. \tag{10}$$

The volumetric flow flux, Q is thus calculated as

$$Q = 2\pi \int_0^{R(z)} r \, u \, dr$$

$$= -\frac{\pi R_0^4}{8\mu} \frac{dp}{dz} (R/R_0)^4 \left\{ 1 - \frac{4\sqrt{D_a}}{\alpha R_0^2 (R/R_0)^2} \left\{ R_0 (R/R_0) - 2\alpha \sqrt{D_a} \right\} \right\}. \tag{11}$$

From equation (11), one now obtains

$$-\frac{dp}{dz} = \frac{8\mu Q}{\pi R_0^4}\phi(z),\tag{12}$$

with

$$\phi(z) = 1/F(z), \quad F(z) = (R/R_0)^4\left\{1 - \frac{4\sqrt{D_a}}{\alpha R_0^2 (R/R_0)^2}\left\{R_0(R/R_0) - 2\alpha\sqrt{D_a}\right\}\right\}.$$

The pressure drop, Δp (= p at $z = 0, - p$ at $z = L$) across the stenosis in the tube of length, L is derived as

$$\begin{aligned}\Delta p &= \int_0^L\left(-\frac{dp}{dz}\right)dz \\ &= \frac{8\mu Q}{\pi R_0^4}\psi,\end{aligned}\tag{13}$$

where

$$\psi = \int_0^d[\phi(z)]_{R/R_0 = 1}\,dz + \int_d^{d+L_0/2}[\phi(z)]_{R/R_0\ from\ (1)}\,dz + \int_{d+L_0/2}^{d+L_0}[\phi(z)]_{R/R_0\ from\ (2)}\,dz + \int_{d+L_0}^L[\phi(z)]_{R/R_0 = 1}\,dz.$$

The first and the fourth integrals in the expression for ψ obtained above are straight forward whereas the analytical evaluation of second and third integrals are almost a formidable task and therefore shall be evaluated numerically.

The flow resistance (resistive impedance), $\overline{\lambda}$, the wall shear stress, $\overline{\tau}_w$ and the shearing stress at the stenosis throat (located at $z = d + L_0/2$), $\overline{\tau}_s$ are now calculated as

$$\overline{\lambda} = \frac{\Delta p}{Q} = \frac{8\mu}{\pi R_o^4}\,\psi,\tag{14}$$

$$\overline{\tau}_w = -\frac{R}{2}\frac{dp}{dz} = \frac{4\mu Q}{\pi R_o^3}(R/R_0)\phi(z),\tag{15}$$

$$\overline{\tau}_s = \frac{4\mu Q}{\pi R_o^3}[(R/R_0)\phi(z)]_{R/R_0 = 1 - \delta/R_0}.\tag{16}$$

Following now the reports of Srivastava and Rastogi (2009, 2010a), one derives the expressions for the impedance (flow resistance), λ, the wall shear stress distribution in the stenotic region, τ_w and shearing stress at the stenosis throat, τ_s in their non-dimensional form as

$$\lambda = 1 - L_o/L + \frac{\eta}{L} \int_d^{d+L_0/2} \frac{dz}{a^4 \left[1 - \frac{4\sqrt{D_a}}{\alpha R_0^2 a^2} \left\{ R_0 a - 2\alpha\sqrt{D_a} \right\} \right]}$$

$$+ \frac{\eta L_0}{2\pi L} \int_0^\pi \frac{d\beta}{\theta^4 \left[1 - \frac{4\sqrt{D_a}}{\alpha R_0^2 \theta^2} \left\{ R_0 \theta - 2\alpha\sqrt{D_a} \right\} \right]} , \qquad (17)$$

$$\tau_w = \frac{\eta}{\left\{ (R/R_0)^3 - \frac{4\sqrt{D_a}}{\alpha R_0^2} \left\{ R_0 (R/R_0)^2 - 2\alpha\sqrt{D_a} \ (R/R_0) \right\} \right\}} , \qquad (18)$$

$$\tau_s = \frac{\eta}{\left\{ (1 - \delta/R_0)^3 - \frac{4\sqrt{D_a}}{\alpha R_0^2} \left\{ R_0 (1 - \delta/R_0)^2 - 2\alpha\sqrt{D_a} \ (1 - \delta/R_0) \right\} \right\}} , \qquad (19)$$

where

$$a \approx a(z) = 1 - 2\delta(z - d)/R_0 L_0 ; \ b = 1 - \delta/2R_0 ; \ c = -\delta/2R_0$$

$$\theta \approx \theta(\beta) = b + c \cos\beta \ ; \beta = \pi - (2\pi/L_0)(z - d - L_0/2), \ \eta = 1 - \frac{4\sqrt{D_a}}{\alpha R_0^2} \left\{ R_0 - 2\alpha\sqrt{D_a} \right\},$$

$\lambda = \bar{\lambda}/\lambda_0$, $(\tau_w, \tau_s) = (\bar{\tau}_w, \bar{\tau}_s)/\tau_0$, $\lambda_0 = 8\mu L / \pi \eta R_0^4$, $\tau_0 = 4\mu Q / \pi \eta R_0^3$ are the flow resistance and shear stress, respectively for a Newtonian fluid in a normal artery (no stenosis).
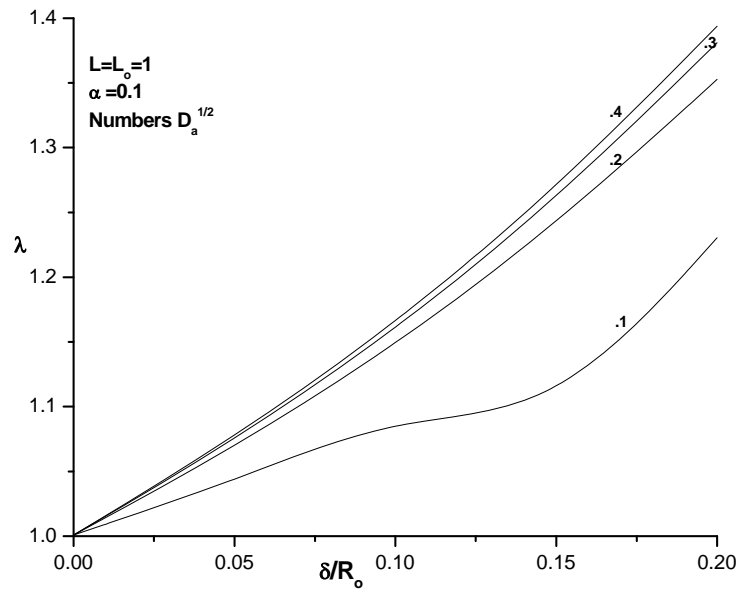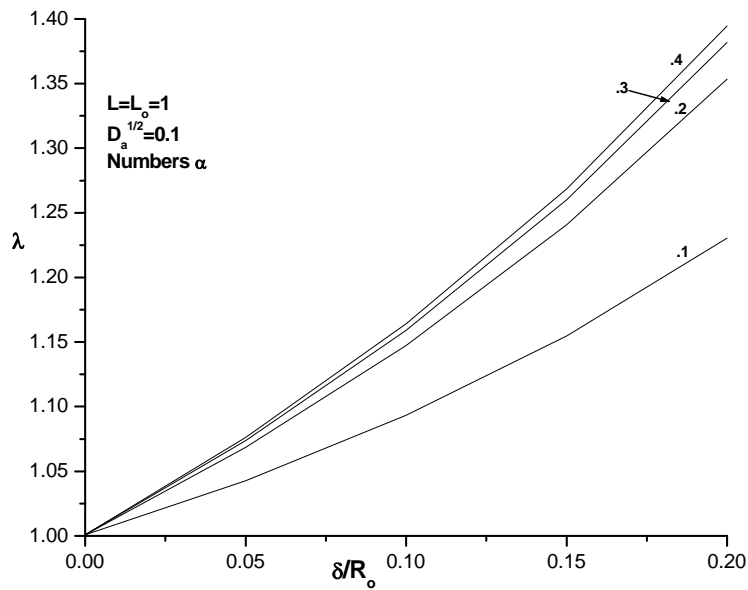
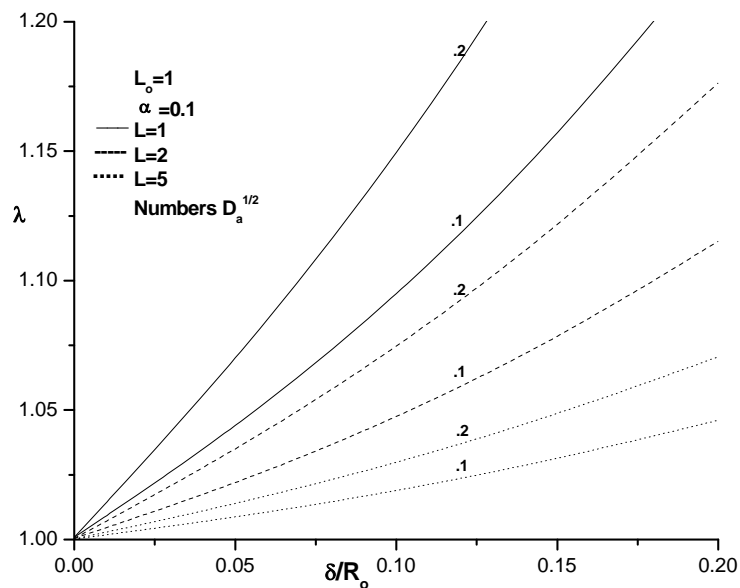**Fig.2 Impedance, λ versus stenosis height, δ/R_o for different Darcy number, $D_a^{1/2}$.**

4.   Numerical Results and Discussion

In order to have an estimate of the quantitative effects of the various parameters involved in the analysis, computer codes are developed to evaluate the analytical results obtained for dimensionless resistance to flow, λ, the wall shear stress, τ_w in the stenotic region and the shearing stress at stenosis throat, τ_s [equations (17-19] in a tube of radius 0.01 cm for parameter values: $d = 0$; $L_0 \text{(cm)} = 1$; $L \text{(cm)} = 1, 2, 5$ $\alpha = 0.1, 0.2, 0.3, 0.4$; $\sqrt{D_a} = 0.1, 0.2, 0.3, 0.4$; $\delta/R_0 = 0$, 0.05, 0.10, 0.15, 0.20.

The impedance (flow resistance), λ increases with increasing values of the Darcy number, $\sqrt{D_a}$ (square root of the Darcy number and hereafter referred as the Darcy number) for a given value of slip parameter, α and any stenosis height, δ/R_0 (Figure 2). One notices that the blood flow characteristic, λ increases with the slip parameter, α for a given value of Darcy number, $\sqrt{D_a}$ (Figure 3). For a given Darcy number, $\sqrt{D_a}$, the impedance, λ decreases with increasing tube length, L for any given value of the slip parameter, α which interns implies that λ increases with stenosis length L_0 (Figure 4). The blood flow characteristic, λ also increases with stenosis size, L_0 for a given Darcy number, $\sqrt{D_a}$ and for any value of the slip parameter, α (Figure 5). For any given stenosis height, δ/R_0 the flow resistance, λ decreases with increasing

Fig.3 Impedance, λ versus stenosis height, δ/R_o for different slip parameter, α.

Fig.4 Impedance, λ versus stenosis height, δ/R_o for different tube length, L and Darcy number, $D_a^{1/2}$.

Darcy number, $\sqrt{D_a}$ for a given slip parameter α and assumes an asymptotic magnitude at $\sqrt{D_a} = 0.15$ for a given value of the slip parameter, α (Figure 6). However, for a given Darcy number, $\sqrt{D_a}$, λ increases with the slip parameter and assumes an asymptotic magnitude at about $\alpha = 0.25$ for any given stenosis height, δ/R_0 (Figure 7).
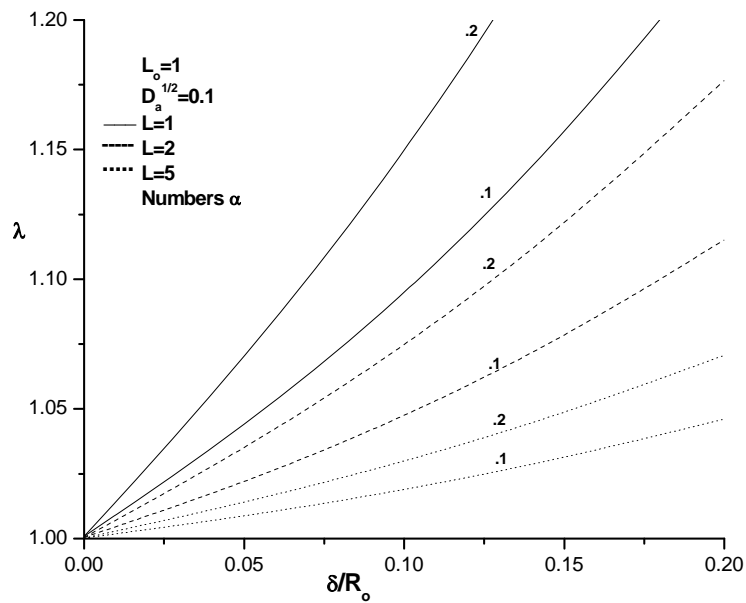
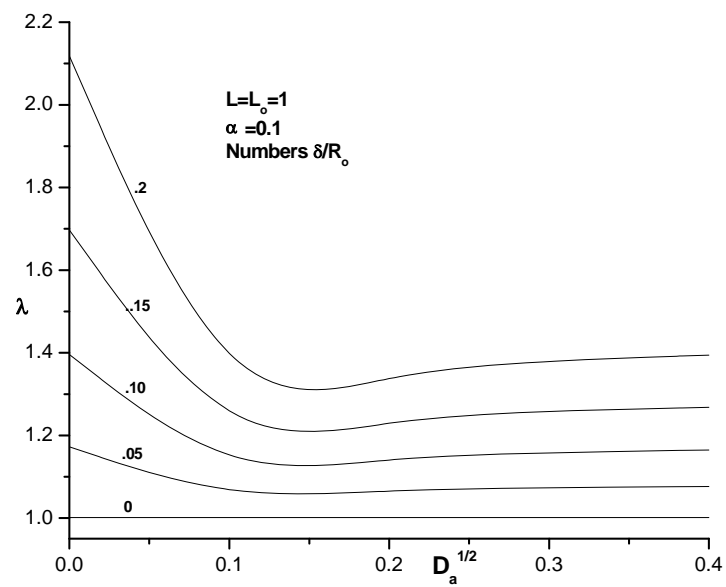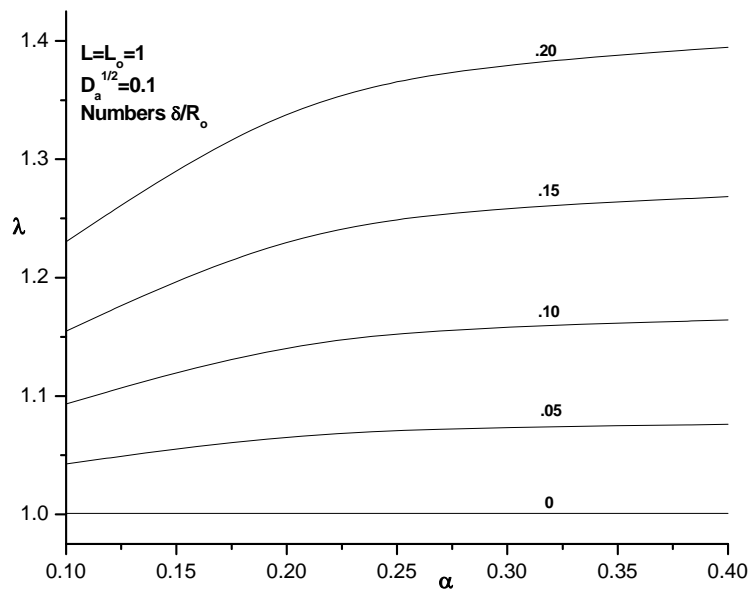**Fig.5 Impedance, λ versus stenosis height, δ/R$_o$ for different tube length, L and slip parameter, α.**

Fig.6 Impedance, λ versus Darcy number, D$_a$$^{1/2}$ for different stenosis height, δ/R$_o$.

**Fig.7 Impedance, λ versus slip parameter, α for different
stenosis height, δ/R$_o$.**

Finally, to have an exact estimate of the effects of the Darcy number and the slip parameter on the flow characteristics due to the presence of a stenosis. Some of the results are summarized in Tables 1 and 2. We observe that the impedance increases with the Darcy number $\sqrt{D_a}$ and the slip parameter, α. However, for increasing values of any of these parameters ($\sqrt{D_a}$ or α), the impedance attains significantly higher magnitude in stenosed artery than a normal artery. In particular, for $\alpha = 0.1$ and $\delta/R_0 = 0.1$ (i.e., 19% stenosis by area reduction). The percentage increase in the magnitude of λ is 9.22% and 13.90% respectively for $\sqrt{D_a} = 0.1$ and 0.2. The percentage increase in λ for $\alpha = 0.1$ and $\delta/R_0 = 0.15$ (28% stenosis) is 15.38% and 23.94% ,

Table 1. Variations of λ and τ_s for $\alpha = 0.1$ and different $\sqrt{D_a}$ and δ/R_0.

δ/R_0	$\sqrt{D_a}$			
	0.1		0.2	
	λ	τ_s	λ	τ_s
0.00	1.0009	1.0000	1.0009	1.0000
0.05	1.0426	1.0029	1.0684	1.0354
0.10	1.0932	1.0108	1.1472	1.0754
0.15	1.1548	1.0240	1.2405	1.1206
0.20	1.2348	1.0429	1.3529	1.1721

Respectively, for $\sqrt{D_a}$ = 0.1 and 0.2. Likewise, for $\sqrt{D_a}$ = 0.1 and δ/R_0= 0.1, the percentage increase in λ is 14.62% and 16.30%, respectively, for α = 0.1 and 0.2. The percentage increase in λ for $\sqrt{D_a}$ = 0.1 and δ/R_0= 0.15 is 23.97% and 26.71%, respectively, for α = 0.1 and 0.2.

Table 2. Variations of λ and τ_s for $\sqrt{D_a}$ = 0.1 and different α and δ/R_0

| δ/R_0	α				
	0.1			0.2	
	λ	τ_s		λ	τ_s
0.00	1.0009	1.0000		1.0009	1.0000
0.05	1.0685	1.0356		1.0761	1.0452
0.10	1.1474	1.0757		1.1640	1.0955
0.15	1.2408	1.1210		1.2682	1.1519
0.20	1.3534	1.1727		1.3940	1.2154
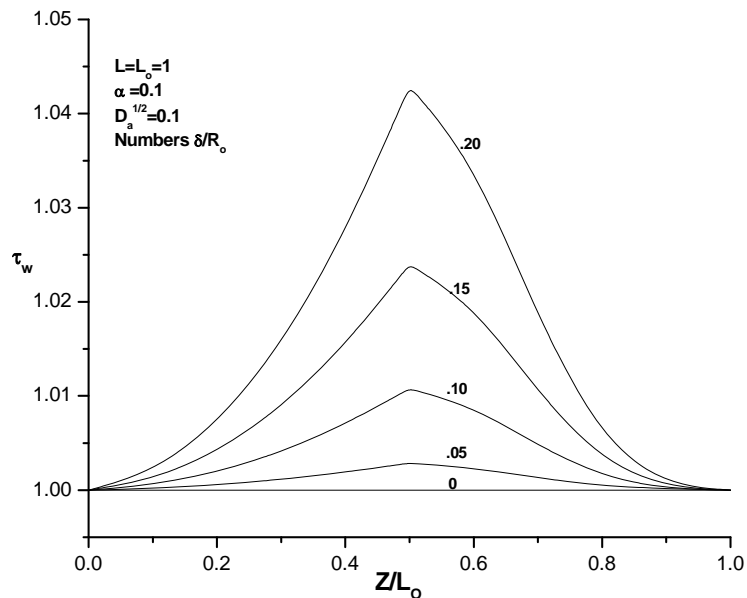
Fig.8 Wall shear stress, τ_w distribution in the stenotic region for different stenosi height, δ/R_o.

The non-dimensional wall shear stress, τ_w increases with stenosis height, δ/R_0 at any axial distance z/L_0 for a given value of slip parameter, α and the Darcy number, $\sqrt{D_a}$. τ_w increases from its approached magnitude at $z/L_0 = 0$ to its peak value at the stenosis throat at $z/L_0 = 0.5$ and then decreases from its value at the throat to its approached magnitude at end point of the constriction profile (Figure 8). The blood flow characteristic τ_w also increases with the Darcy

number, $\sqrt{D_a}$ at any axial distance z/L_0 (Figure 9). One observes that in the stenotic region, $0 \le z/L_0 \le 1$, τ_w increases with the slip parameter, α for any given stenosis height δ/R_0 and the Darcy number, $\sqrt{D_a}$ (Fig. 10).
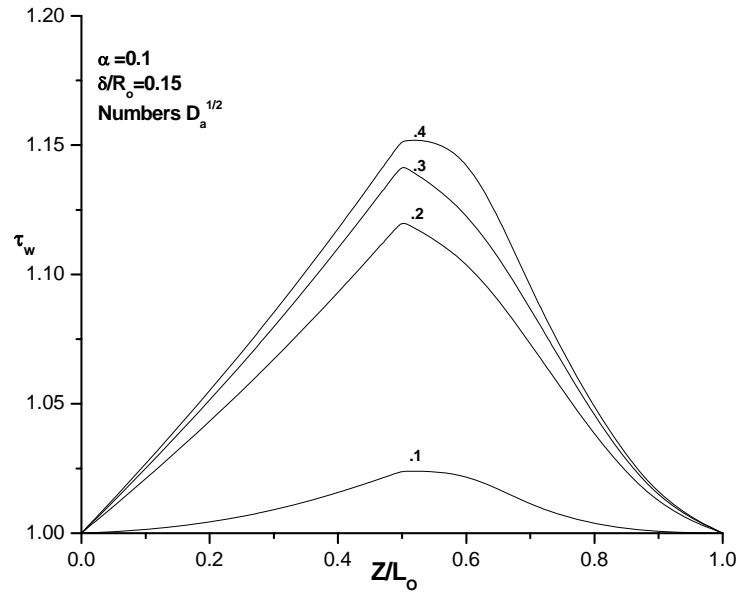
Fig.9 Wall shear stress, τ_w distribution in the stenotic region for different Darcy numbe, $D_a^{1/2}$.
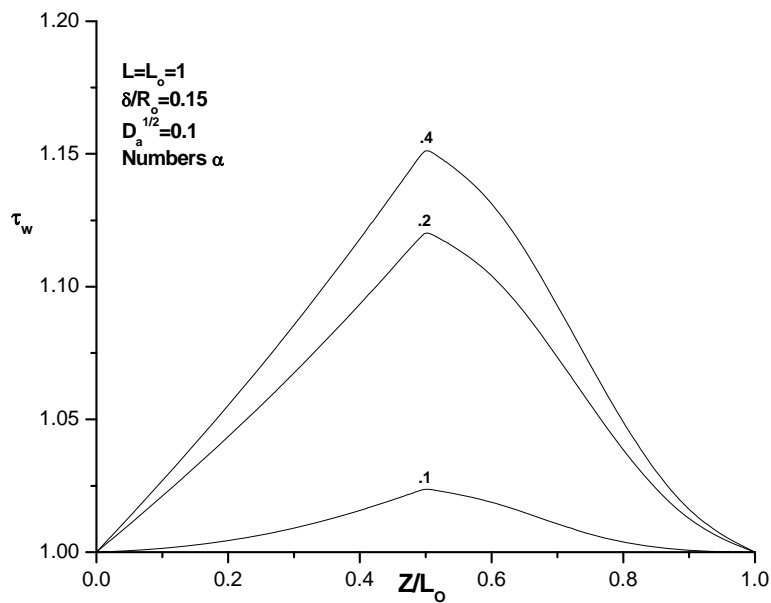
Fig.10 Wall shear stress, τ_w distribution in the stenotic region for different slip parameter, α .
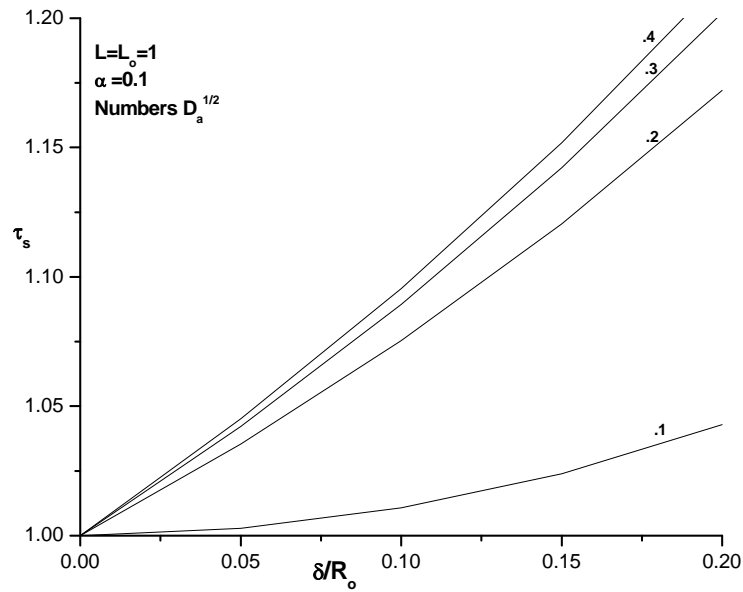
Fig.11 Shear stress at stenosis throat, τ_s versus stenosis height, δ/R_o for different Darcy number, $D_a^{1/2}$.
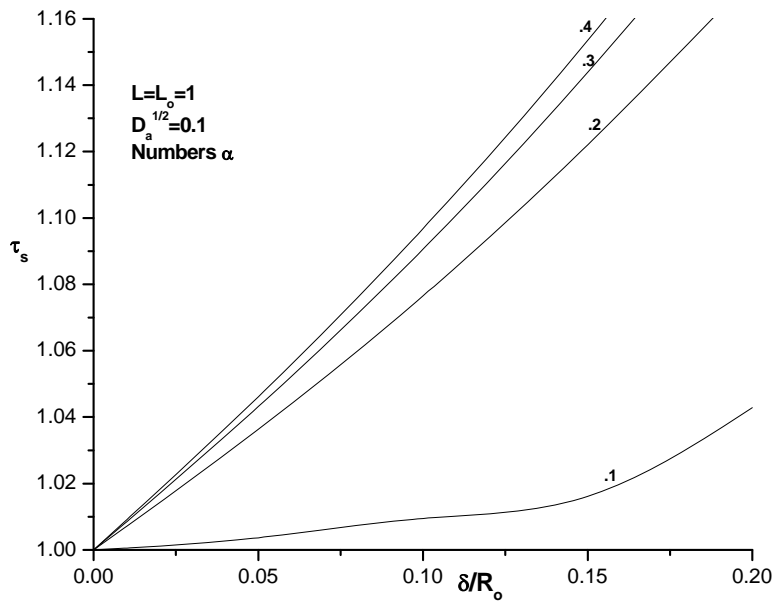

Fig.12 Shear stress at stenosis throat, τ_s versus stenosis height, δ/R_o for different slip parameter, α.

It is interesting to note that the nature of the variations of τ_w remains similar with respect to any of the parameters, δ/R_0, α and $\sqrt{D_a}$ (Figures 8-10).

The shear stress at stenosis throat τ_s increases with the Darcy number, $\sqrt{D_a}$ for any given value of the slip parameter α and the stenosis height δ/R_0 (Figure 11). The flow characteristic τ_s is observed to be increasing with the slip parameter, α for any given Darcy number, $\sqrt{D_a}$ and stenosis height δ/R_0 (Figure 12). The nature of the variations of shear stress at stenosis throat τ_s is found to be similar to that of the impedance, λ with respect to any parameter (Figures 2, 3, 11, and 12).

5. Conclusions

To observe the effects of wall permeability on blood flow characteristics in a stenosed artery, the flow of a Newtonian fluid through a composite stenosis in a circular tube with permeable wall has been discussed. The impedance increases with the Darcy number as well as with the slip parameter. The flow resistance also increases with the stenosis size (height and length both) for any given set of parameters. On the basis of the results summarized in Tables 1 and 2, it is concluded that the impedance assumes significantly higher magnitude in a permeable stenosed artery than its corresponding value in a normal artery (no stenosis). The shear stress at the stenosis throat possesses characteristics similar to the impedance with respect to any parameter.

REFERENCES

Ahmed, A. S. and Giddens, D. P. (1983). Velocity measurements in steady flow through axisymmetric stenosis at moderate Reynolds number. J. of Biomech, 16, pp. 505-516.

Beavers, G.S. and Joseph, D. D. (1967). Boundary conditions at a naturally permeable wall. J. Fluid Mech. 30(1), pp. 197-207.

Caro, C. G. Pedley, T. J., Schroter, R.C. and Seed, W. A. (1978). The Mechanics of the Circulation. Oxford Medical, N. Y.

Joshi, P., Pathak, A. and Joshi, B.K. (2009). Two layered model of blood flow through composite stenosed artery, Applications and Applied Mathematics, 4(2), pp. 343-354.

Jung. H. Choi, J.W. and Park, C.G. (2004). Asymmetric flows of non-Newtonian fluids in symmetric stenosed artery. Korea-Aust, Rheol. Journal, 16, pp. 101-108.

Layek, G.C., Mukhopadhyay, S. and Gorla, R.S.R. (2009). Unsteady viscous flow with variable viscosity in a vascular tube with an overlapping constriction, Int. J. Engg. Sci., 47, pp. 649-659.

Layek, G.C., Mukhopadhyay, S. and Samad, Sk. A. Oscillatory flow in a tube with multiple constrictions, Int. J. Fluid Mech. Res., 32, pp. 402-419, 2005.

Liu, G.T., Wang, X.J., Ai, B.Q. and Liu, L.G. (2004). Numerical study of pulsating flow through a tapered artery with stenosis, Chin. Journal Phys., 42, pp. 401-409.

Mandal, P.K. (2005). An unsteady analysis of non-Newtonian blood flow through tapered arteries with a stenosis, Int. J. of Nonlinear Mech., 40, pp. 51–164.

Mandal, P.K., Chakravarty, S. and Mandal, A. (2007a). Numerical study on the unsteady flow of non-Newtonian fluid through differently shaped arterial stenosis, Int. J. Comput. Math., 84, pp. 1059-1077.

Mandal, P.K., Chakravarty, S., Mandal, A. and Amin, A. (2007b). Effect of body acceleration on unsteady pulsatile flow of non-Newtonian fluid through a stenosed artery, Appl. Math. Comput., 189, pp. 766-779.

Mann, F. C., Herrick, J. F., Essex, H. E. and Blades, E. J. (1938). Effects on blood flow of decreasing the lumen of blood vessels. Surgery, 4, pp. 249-252.

Mekheimer, Kh. S. and El-Kot, A. M. E. (2008). Magnetic field and hall currents influences on blood flow through a stenotic arteries, Applied Mathematics and Mechanics, 29, pp. 1-12.

Mishra, B. K. and Verma, N. (2007). Effects of porous parameter and stenosis on the wall shear stress for the flow of blood in human body, Res. J. medicine and Medical Sciences, 2, pp. 98-101.

Misra, J.C. and Shit, G.C. (2006). Blood flow through arteries in a pathological state: A theoretical study. Int. J. Engg. Sci., 44, pp. 662-671.

Politis, A. K., Stavropoulos, G. P., Christolis, M. N., Panagopoulos, F. G., Vlachos, N. S., and Markatos, N. C. (2007). Numerical modeling of simulated blood flow in idealized composite arterial coronary grafts: Steady state simulations. J. Biomech., 40(5), pp. 1125–1136.

Politis, A. K., Stavropoulos, G. P., Christolis, M. N. Panagopoulos, F. G., Vlachos, N. S. and Markatos, N. C. (2008). Numerical modeling of simulated blood flow in idealized composite arterial coronary grafts: Transient flow. J. Biomech., 41(1), pp. 25-39.

Ponalagusamy, R. (2007). Blood flow through an artery with mild stenosis: A two layered model, different shapes of stenosis and slip velocity at the wall. J Appl. Sci., 7(7), pp. 1071-1077.

Pralhad, R.N. and Schultz, D.H. (2004). Modeling of arterial stenosis and its applications to blood diseases. Math. Biosci. 190, pp. 203-220.

Sarkar, A. and Jayaraman, G. (1998). Corretion to flow rate-pressure drop in coronary angioplasty; steady streaming effect, Journal of Biomech. 31, pp. 781-791.

Shukla, J. B., Parihar, R. S. and Gupta, S. P. (1980). Effects of peripheral layer viscosity on blood flow thorough the artery with mild stenosis. Bull. Math. Biol., 42, pp. 797-805.

Singh, B., Joshi, P. and Joshi, B.K. (2010). Blood flow through an artery having radially non-summetric mild stenosis. Appl. Math. Sci., 4(22), pp. 1065-1072.

Srivastava, V. P. and Rastogi, R. (2010a). Blood flow through stenosed catherterized artery: effects of hematocrit and stenosis shape, Comput. Math. Applc. 59, pp. 1377-1385.

Srivastava, V.P. (1996). Two-phase Model of Blood Flow through Stenosed Tubes in the Presence of a Peripheral Layer: J. Biomech., 29, pp. 1377-1382.

Srivastava, V. P. and Rastogi, R. (2009). Effects of hematocrit on impedance and shear stress during stenosed artery catheterization, Applications and Applied Mathematics, 4, pp. 98-113.

Srivastava, V.P., Vishnoi, Rochana and Sinha, P. (2010c). Particulate Suspension Blood Flow through a Stenosed Catheterized Artery, Applications and Applied Mathematics, 5, pp. 1352-1368.

Srivastava, V.P., Vishnoi, Rochana, Mishra, Shailesh and Sinha, P. (2010b). Blood flow through a composite stenosis in catheterized arteries, e- J. Sci. Tech., 5, pp. 55-64.

Tzirtzilakis, E.E. (2008). Biomagnetic fluid flow in a channel with stenosis, Physica, D 237, pp. 66-81.

Young, D. F. and Tsai, F. Y. (1973). Flow characteristics in model of arterial stenosis – steady flow, Journal of Biomech. 6, pp. 395-410.

Young, D. F. (1968). Effects of a time-dependent stenosis of flow through a tube, Journal of Eng. Ind., 90, pp. 248-254.

Young, D. F. (1979). Fluid mechanics of arterial stenosis, J. Biomech. Eng. ASME, 101, pp. 157-175.